Nihon Reoroji Gakkaishi Vol.37, No.4, 191~198
(Journal of the Society of Rheology, Japan)

Article

Improvement of Thixotropy Model Analyzing Dispersion Characteristics of Fine Particles in Newtonian Molten Polymer

Emi HASEGAWA, Hiroshi SUZUKI, Yoshiyuki KOMODA, and Hiromoto USUI

Department of Chemical Science and Engineering, Graduate School of Engineering, Kobe University
1-1, Rokkodai-cho, Nada-ku, Kobe, Hyogo 657-8501, Japan
(Received : March 30, 2009)

A model estimating the time-dependent distribution of cluster size consisting of fine particles in Newtonian molten polymer has been improved. The present model for agglomerative suspension was developed based on Usui's thixotropy model, derived by taking the balance between shear breakup, shear coagulation and Brownian coagulation process. The interparticle bonding energy in the model was assumed as a function of a cluster size in this study though it was assumed to be constant in the previous study. The analysis was applied to the experimental results for silica/(ethylene methyl-meta acrylate copolymer) suspensions. The time variation of cluster size distributions, of viscosities and of the mean number of particles in a cluster was calculated and the results were compared with experimental results mainly for the cases of the solid volume fractions from 0.10 to 0.25 when the shear rate was changed from 0.2 to 10 s^{-1}. From the results, it was found that the present model could estimate well the time dependency of cluster size distributions in a wide range of shear rate when the solid volume fraction was set at 0.15, and that the effect of the solid volume fraction was also sufficiently explained by the present model.
Key Words: Particle agglomeration / Cluster size distribution / Thixotropy model / Dispersion / Shear breakup

1. INTRODUCTION

Dispersion characteristics of fine particles in solid-liquid slurries or suspensions are of importance in many industrial processes. The particles in solid-liquid slurries or suspensions coagulate due to the particle's contact by the Brownian motions, the particle velocity difference induced by the fluid flow and by the other external forces, and so on. Smoluchowski[1] worked out the basic theory of the coagulation of the particles in such solid-liquid slurries or suspensions. Swift and Friedlander[2], and Friedlander and Wang[3] investigated theoretically and experimentally the simple shear coagulation in which Brownian coagulation occurs simultaneously. Higashitani et al.[4-6] also investigated the coagulation model and examined the validity of their model experimentally. On the other hand, Parker, Kaufman, and Jenkins[7] investigated the breakup mechanism in shear flows and showed the breakup mechanisms of surface erosion and splitting of a parent aggregate. Sonntag and Russel[8] suggested the relations between the floc size and the deformation rate experimentally. Among them, Usui[9] established a simple model considering Brownian and shear coagulations and shear breakup of clusters, in order to estimate apparent viscosity and bulk agglomeration characteristics of fine particle suspensions when the parent cluster of particles is splitting into smaller fragments by shear addition. It was developed for multi-modal systems (Usui et al.[10]) and applied to many kinds of suspensions (Usui et al.[11], Mustafa et al.[12]). Komoda et al.[13] also revealed it can estimate solid-air systems. Kobayashi et al.[14] also developed shear breakup theory separately.

However, these models assumed cluster size tends to be uniform with while the particles are coagulating and breaking up. In actual cases, the size of clusters including fine particles is widely distributed. Such distribution characteristics severely affect the functions and physical properties of some materials. On this, Komoda et al.[15] experimentally investigated cluster distribution characteristics of fine particles in Newtonian molten polymer in order to clarify a shear breakup process of clusters. Komoda et al.[16] also discussed about the appearance of the viscoelasticity of the suspension in spite of the fact that the disperse media was Newtonian in the case without particles.

In the previous study[17], a model estimating the time-dependent distribution of cluster size consisting of fine spherical particles in Newtonian fluids will be suggested on the silica/EMMA suspension which various shear rates added to. Its trial was partially succeeded but it had some serious errors on the

E-mail: hero@kobe-u.ac.jp

evaluation of dispersion characteristics especially when shear rate was high. This is because the cluster size becomes too small out to the assumption that the cluster has a sphere shape.

In this paper, the model estimating the dispersion characteristics of the silica/EMMA suspensions is improved. The results will be compared with their experimental data and the previous estimation. In this study, the effect of solid volume fraction is also focused on. From this, the present model will be evaluated.

2. MODEL ANALYSIS

2.1 Thixotropy Model

Usui[9] suggested a thixotropy model for analyzing suspension rheological characteristics as follows.

$$\frac{dk}{dt}=\frac{4\alpha_b k_b T N_0}{3\eta_0}+\frac{4\alpha_s \phi_0 k\dot{\gamma}}{\pi}-\frac{3\pi\ {}^{3}_{0}}{4F_0 N_b}\left(\frac{k}{1-\varepsilon}-1\right)\eta\dot{\gamma}^2 \quad (1)$$

Here, t[s], k[-], k_b[J·K^{-1}], T[K], N_0[m^{-3}], ϕ_0[-], ε[-], d_0[m], η[Pa·s], η_0[Pa·s] and $\dot{\gamma}$ [s^{-1}] are time, the number of particles in a cluster, Boltzmann constant, absolute temperature, total number of particles in a unit volume, apparent solid volume fraction, void fraction in a cluster, diameter of particles, slurry viscosity, solvent viscosity and shear rate. α_b[-] and α_s[-] are rate constants of Brownian coagulation and of shear coagulation obtained by Higashitani et al..[4,5] F_0[J] and N_b[-] are the bonding energy and the number of bonds to be broken when the cluster is divided into two clusters. Usui[9] suggested the estimation of the number of bonds under some assumptions as follows.

$$N_b=\frac{kd_0}{2d_k} \quad (2)$$

Here, d_k[m] is the cluster diameter including k particles.

This viscosity was estimated by Simha's cell model in the previous studies.[9-12] Simha[18] gave the following viscosity equation for a mono-modal dense suspension.

$$\frac{\eta}{\eta_0}=1+2.5\lambda(\gamma)\phi \quad (3)$$

Where γ[-] and ϕ[-] are the ratio of the radius of spherical particle to the cell radius, and apparent volume fraction. The function $\lambda(\gamma)$ is given as follows.

$$\lambda(\gamma)=\frac{4\left(1-\gamma^7\right)}{4\left(1+\gamma^{10}\right)-25\gamma^3\left(1+\gamma^4\right)+42\gamma^5} \quad (4)$$

Simha proposed a model that the cell radius was proportional to the difference between the average distance of particles and particle radius. Defining f[3][-] as the supposed volume fraction of total cell, the following relationship is obtained for the case of dense suspension system.

$$\gamma^3=\frac{\phi}{f^3\left[1-\left(\phi^{1/3}/f\right)\right]^3} \quad (5)$$

When the solid volume fraction is the same as the maximum packing volume fraction, $\phi_{p,max}$[-], γ becomes unity, and $\phi_{p,max}=f^3/8$.

When the apparent viscosity of a dense suspension is experimentally determined, the value of k is assumed as the first step. Thus, the void fraction in a cluster is calculated as follows.

$$\varepsilon=\varepsilon_{max}\left(1-k^{-0.4}\right) \quad (6)$$

Here, ε_{max}[-] is the maximum void fraction as follows.

$$\varepsilon_{max}=1-\frac{\phi_0}{\phi_{p.max}} \quad (7)$$

In this study, the cluster diameter, d_k, was estimated as follows.

$$d_k=d_0\left(\frac{k}{1-\varepsilon}\right)^{\frac{1}{3}} \quad (8)$$

Apparent void fraction, ϕ, can be evaluated with the cluster diameter.

$$\phi=\sum_k \frac{\pi}{6}d_k^{\ 3}n_k \quad (9)$$

Here, n_k[m^{-3}] is the concentration of k cluster.

In the Usui's model, the cluster size, k, was decided as the viscosity obtained by experiments agreed with the Simha's estimation. Then, the validation of Simha's model has not yet been discussed enough because the cluster size were not known in the previous studies. Figure 1 shows the comparison of the viscosities obtained by Simha's model and by experiments in the case at the shear rate of 1 s^{-1}. The viscosities estimated by classical Einstein's model[19] and Eilers' model[20] for dense slurries shown in the followings are also plotted.

$$\frac{\eta}{\eta_0}=1+2.5\phi \quad (10)$$

$$\frac{\eta}{\eta_0}=\left(1+\frac{1.25\phi}{1-\phi/\phi_{p,max}}\right)^2 \quad (11)$$

Eilers set 0.74 as $\phi_{p,max}$.

From this, it is found that the viscosity estimated by Simha's model shows much larger values than experimental data. This does not indicate Simha's model is always negative for estimating suspension viscosities, because the over-estimation might be due to the present model calculating

cluster size. However, the over-estimation of the viscosity causes the faster break-up of cluster as reported in the previous study. From the figure, it is also found that the viscosity estimated by Eilers' model shows slightly higher than the experimental data in high volume fraction region, but does the rather agreement with the present experiments. In this study, the Eilers' model was adopted for evaluating the viscosity in order to prevent the over-estimation of viscosity.

Usui's model was established under an assumption that the number of particles in a cluster tends to be uniform. This assumption is also adopted by Swift and Friedlander[2] and Higashitani et al.[4,5] in their analyses. However, the cluster size is widely distributed in an actual suspension as reported by Komoda et al.[15] In such a case, Smoluchowski's traditional coagulation model[1] as shown in the following is required.

$$\frac{dn_k}{dt} = \frac{1}{2}\sum_{\substack{i=1 \\ i+j=k}}^{i=j-1} b_{ij}\cdot n_i n_j - \sum_{i=1}^{\infty} b_{ij}\cdot n_i n_k \qquad (12)$$

Here, n_k[m^{-3}] is the concentration of the clusters composed of k particles. b_{ij} [m^{3}s^{-1}] is rate of Brownian or shear coagulation. According to Smoluchowski's theory[1], b_{ij} can be expressed with rate constant, α_b or α_s as follows for each Brownian or shear coagulation.

$$b_{ij} = \frac{2k_bT\alpha_b}{3\mu}\left(r_i + r_j\right)\left(\frac{1}{r_i}+\frac{1}{r_j}\right)$$

: Brownian coagulation (13)

$$b_{ij} = \frac{4\dot{\gamma}\alpha_s}{3}\left(r_i + r_j\right)^3$$

: shear coagulation (14)

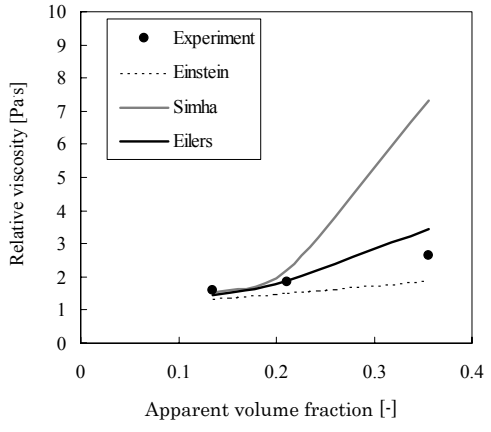

Fig. 1. Relative viscosity at shear rate of 1 s^{-1}.

Here, r_i[m] and r_j[m] are radii of the clusters including i and j particles, respectively.

The shear breakup model of clusters can be developed from Usui's model.[9] In the model, a cluster is assumed to be separated to two clusters, whose total have the same volume as that of the original cluster. Then, the concentration of k cluster is decreased by such a mechanism and is increased by the breakup of the cluster including twice particles, 2k. We also assumed that an even cluster breaks into two equal size clusters but that an odd cluster breaks into two clusters including (k+1)/2 and (k-1)/2 particles, respectively. Then, the breakup rate by shear addition can be obtained as follows.

$$\begin{aligned}\frac{dn_k}{dt} = &-\frac{3}{4}\frac{\pi\cdot\dot{\gamma}^2}{F_0N_b}\frac{\eta\cdot d_0^3}{(k-1)}\left(\frac{k}{1-\varepsilon}-1\right)n_k \\ &+\frac{3}{2}\frac{\pi\cdot\dot{\gamma}^2}{F_0N_b}\frac{\eta\cdot d_0^3}{(2k-1)}\left(\frac{2k}{1-\varepsilon}-1\right)n_{2k} \\ &+\frac{3}{4}\frac{\pi\cdot\dot{\gamma}^2}{F_0N_b}\frac{\eta\cdot d_0^3}{(2k-2)}\left(\frac{2k-1}{1-\varepsilon}-1\right)n_{2k-1} \\ &+\frac{3}{4}\frac{\pi\cdot\dot{\gamma}^2}{F_0N_b}\frac{\eta\cdot d_0^3}{2k}\left(\frac{2k+1}{1-\varepsilon}-1\right)n_{2k+1}\end{aligned} \qquad (15)$$

The final form on the concentration change rate of k cluster can be derived with coagulation terms discussed above as follows.

$$\begin{aligned}\frac{dn_k}{dt} = &\frac{1}{2}\alpha_b\sum_{\substack{i=1 \\ i+j=k}}^{i=j-1}\frac{2k_bT}{3\eta_0}\left(r_i+r_j\right)\left(\frac{1}{r_i}+\frac{1}{r_j}\right)n_in_j-\alpha_b\sum_{i=1}^{\infty}\frac{2k_bT}{3\eta_0}\left(r_i+r_j\right)\left(\frac{1}{r_i}+\frac{1}{r_j}\right)n_in_k \\ &+\frac{1}{2}\alpha_s\sum_{\substack{i=1 \\ i+j=k}}^{i=j-1}\frac{4\dot{\gamma}}{3}\left(r_i+r_j\right)^3n_in_j-\alpha_s\sum_{i=1}^{\infty}\frac{4\dot{\gamma}}{3}\left(r_i+r_j\right)^3n_in_k \\ &-\frac{3}{4}\frac{\pi\cdot\dot{\gamma}^2}{F_0N_b}\frac{\eta\cdot d_0^3}{(k-1)}\left(\frac{k}{1-\varepsilon}-1\right)n_k+\frac{3}{2}\frac{\pi\cdot\dot{\gamma}^2}{F_0N_b}\frac{\eta\cdot d_0^3}{(2k-1)}\left(\frac{2k}{1-\varepsilon}-1\right)n_{2k} \\ &+\frac{3}{4}\frac{\pi\cdot\dot{\gamma}^2}{F_0N_b}\frac{\eta\cdot d_0^3}{(2k-2)}\left(\frac{2k-1}{1-\varepsilon}-1\right)n_{2k-1}+\frac{3}{4}\frac{\pi\cdot\dot{\gamma}^2}{F_0N_b}\frac{\eta\cdot d_0^3}{2k}\left(\frac{2k+1}{1-\varepsilon}-1\right)n_{2k+1}\end{aligned} \qquad (16)$$

This equation is based on that the energy of N_b bonds were broken simultaneously, when the cluster was separated into two clusters. The bonding energy, F_0, can be assumed to take a constant value as it was assumed in the previous study.[17] However, this shear breaking-up model is based on the assumption that a cluster is spherical. As shown later, this assumption is not always correct when a cluster size is small. In order to correct this effect, we assumed that the bonding energy was a function of cluster size as described later.

2.2 Silica/EMMA Slurry

In this paper, the model analysis has been applied to the experimental data obtained by Komoda et al.[15] Fine particles of silica were dispersed in ethylene methyl-meta acrylate copolymer (EMMA) in their experiments. The diameter of the silica particle ranges from 2.25 to 2.75 μm by experimental measurements, but d_0 is assumed to be uniform at 2.5 μm in the analysis. The viscosity of EMMA, η_0, is 190.5Pa·s at 120 °C and showed a constant shear viscosity independently of shear rate (Newtonian fluid). The volume fraction of silica particles, ϕ_0 [-], was changed from 0.10 to 0.25 in this study though it was set at 0.15 in the previous study.

The constant shear was added to the mixture at 120 °C, which is higher than the melting point of EMMA at 67 °C, by using a stress controlled cone-and-plate type rheometer (SR-5, Rheometric Scientific). The cone fixture has the diameter of 4 cm and the cone angle of 0.04 rad. The initial condition of cluster distribution was obtained by applying shear at the shear rate at 0.1 s^{-1} for 1000 s.

After the establishment of the initial condition, the shear rate applied to the mixture was changed to 1.0 s^{-1} immediately and maintained for a certain time by using the rheometer control software. After the application of shear, the rotation of the cone fixture was stopped and the mixture was cooled down to 25 °C in a several minutes. As a result, the thin film of the mixture, in which particles in various dispersed states depending on shearing conditions were included, was obtained. The thin film peeled from the cone fixture was cut off by using a microtome to observe the cross sectional area. From the scanning electron microscope (SEM) image of the sliced cross-section, the cluster distribution was obtained at 10, 100 and 1000 s after the initial condition.

3. RESULTS AND DISCUSSION

3.1 Boding Energy

In the previous study, the bonding energy between particles was obtained by Usui's original model[9] from a steady-state experimental data as assumed that $dk/dt = 0$ as follows.

$$\frac{4\alpha_b k_b T N_0}{3\eta_0} + \frac{4\alpha_s \phi_0 k\dot{\gamma}}{\pi} - \frac{3\pi d_0^3 k}{4F_0 N_b}\left(\frac{k}{1-\varepsilon} - 1\right)\eta\dot{\gamma}^2 = 0 \quad (17)$$

In this equation, viscosity and shear rate obtained by the experimental data were used, and k was determined as the viscosity calculated by Simha's model[18] was equal to the corresponding experimental one.

Figure 2 shows the bonding energy for each shear rate in each case of solid volume fraction. The bonding energy calculated from the experimental data is not constant and tends to increase with shear rate as shown in the figure. When the shear rate increases, the particle number in a cluster becomes low. Usui et al.[10] pointed out that there exists the limitation of cluster breakup by shear addition and improved their model considering the cluster size limitation. This is considered to correspond to such cluster limitation. Figure 3 shows the ratio of chain like clusters obtained by experiments. Usui's model assumed that all clusters have spherical shapes in its shear break-up term. This figure indicates clusters become chain-like as the number of particles in a cluster decreases. To such a chain-like cluster, a new break-up mechanism of clusters should be taken into account.

Figure 4 shows the calculated boding energy as a function of cluster size, k, from the distribution of cluster size at 1000 s after shear rate change in case when shear rate and solid volume fraction are 10 s^{-1} and 0.15, respectively. In this situation, the distribution of cluster size can be assumed to be in a perfectly steady state. The bonding energy corresponding to each cluster size was calculated as a function of k with the following equation.

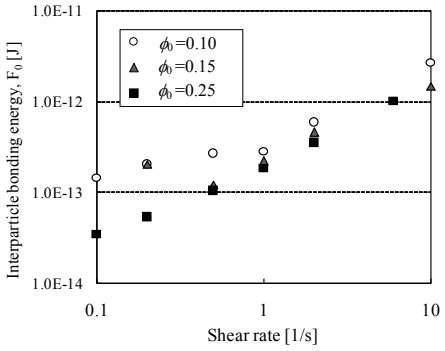

Fig. 2. Interparticle bonding energy calculated from Usui's model.

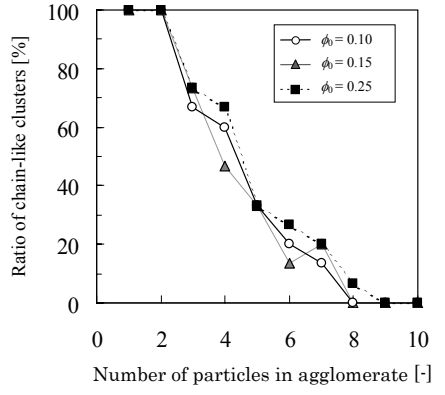

Fig. 3. Ratio of chain-like clusters.

$$\frac{1}{2}\alpha_b\sum_{\substack{i=1\\i+j=k}}^{i=j-1}\frac{2k_bT}{3\eta_0}\left(r_i+r_j\right)\left(\frac{1}{r_i}+\frac{1}{r_j}\right)n_in_j-\alpha_b\sum_{i=1}^{\infty}\frac{2k_bT}{3\eta_0}\left(r_i+r_j\right)\left(\frac{1}{r_i}+\frac{1}{r_j}\right)n_in_k$$
$$+\frac{1}{2}\alpha_s\sum_{\substack{i=1\\i+j=k}}^{i=j-1}\frac{4\dot{\gamma}}{3}\left(r_i+r_j\right)^3n_in_j-\alpha_s\sum_{i=1}^{\infty}\frac{4\dot{\gamma}}{3}\left(r_i+r_j\right)^3n_in_k$$
$$-\frac{3}{4}\frac{\pi\cdot\dot{\gamma}^2}{F_0(k)N_b}\frac{\eta\cdot d_0^3}{(k-1)}\left(\frac{k}{1-\varepsilon}-1\right)n_k+\frac{3}{2}\frac{\pi\cdot\dot{\gamma}^2}{F_0(2k)N_b}\frac{\eta\cdot d_0^3}{(2k-1)}\left(\frac{2k}{1-\varepsilon}-1\right)n_{2k}$$
$$+\frac{3}{4}\frac{\pi\cdot\dot{\gamma}^2}{F_0(2k-1)N_b}\frac{\eta\cdot d_0^3}{(2k-2)}\left(\frac{2k-1}{1-\varepsilon}-1\right)n_{2k-1}$$
$$+\frac{3}{4}\frac{\pi\cdot\dot{\gamma}^2}{F_0(2k+1)N_b}\frac{\eta\cdot d_0^3}{2k}\left(\frac{2k+1}{1-\varepsilon}-1\right)n_{2k+1}=0 \qquad (18)$$

From this, it is found that the bonding energy increases as cluster size decreases. Though the bonding energy should be determined by particle characteristics, the present bonding energy includes the work spent for shear breakup, which depends on the cluster structure. In this paper, the bonding energy was given as a function of cluster size as shown by a solid line in the figure. As the function should be tends to be constant to large clusters, it can be expressed as follows.

$$F_0(k)=5\times10^{-11}k^{-3}+5\times10^{-14}\ \text{J} \qquad (12)$$

In the present model, this function was adopted instead of the average value of 5.0×10^{-13} J used in the previous study[17] as shown as a broken line in the figure.

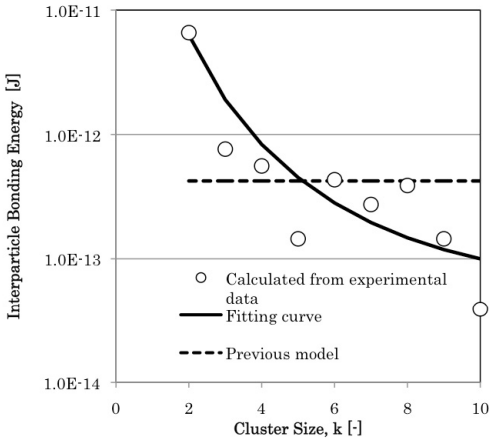

Fig. 4. Bonding energy calculated from cluster size distribution in the case when $\phi_0=0.15$ and $\dot{\gamma}=10\ \text{s}^{-1}$ at 1000 s.

3.2 Validation of the Present Model on the Effect of the Shear Rate

At first, the validation of the present model will be discussed through the comparison with the previous model[17] where the bonding energy was assumed to be constant.

Figure 5(a), (b) and (c) show the time variations of cumulative particle number distribution in a cluster in cases of the shear rates of 0.2, 1, and 10 s^{-1} when $\phi_0=0.15$, respectively. Figure 6(a), (b) and (c) show the time variations of mean cluster size corresponding to the cases.

The mean cluster size becomes low in all cases of shear rates by higher shear addition from the initial state where the shear rate of 0.1 s^{-1} was added. Corresponding to this, the cumulative particle number distribution shifts upper, that is, the frequency of lower cluster size increases. When the shear rate of 0.2 s^{-1}, the cluster size calculated with the previous model is found to become low more slowly than the experimental results. On the other hand, the results of the present model agree well with the experimental results. When the shear rate of 1 s^{-1} is added, the results of the present model also express the experimental data much better than ones obtained by the previous model. In the case of 10 s^{-1}, the mean cluster size computed by the present model becomes small more quickly than experimental results, but the final value well agrees with the experimental one. From these results, it can be concluded that the present model

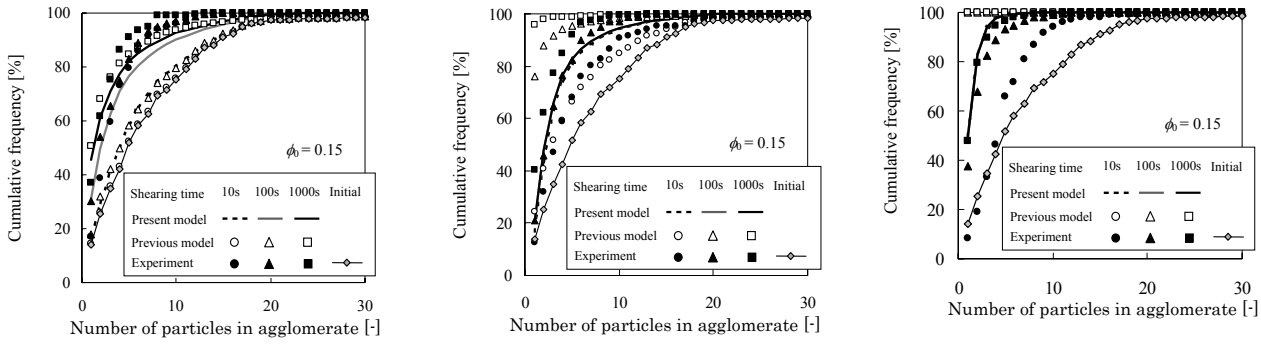

(a) $\dot{\gamma}=0.2\ \text{s}^{-1}$ (b) $\dot{\gamma}=1.0\ \text{s}^{-1}$ (c) $\dot{\gamma}=10\ \text{s}^{-1}$.

Fig. 5. Cumulative cluster size distributions when $\phi_0=0.15$ (a) $\dot{\gamma}=0.2\ \text{s}^{-1}$, (b) $\dot{\gamma}=1.0\ \text{s}^{-1}$, (c) $\dot{\gamma}=10\ \text{s}^{-1}$.

improvement is valid when $\phi_0 = 0.15$.

In the next section, the effect of volume fraction will be discussed with the present model.

3.3 Effect of Volume Fraction

Figure 7(a) and (b) show the time variations of cumulative particle number distribution in a cluster in cases when $\phi_0 = 0.10$ and 0.25 at the shear rates of 1 s^{-1}, respectively. Figure 8(a) and (b) show the time variations of mean cluster size in cases of the corresponding volume fraction. In these figures, both results obtained experimentally and analytically are plotted.

From these figures, it is found that the mean cluster size in the case when $\phi_0 = 0.10$ shows higher value than one of experimental result. Corresponding to this, the change of cumulative cluster size distribution stops at 100s. On the other hand, when $\phi_0 = 0.25$, the cluster size shows good agreements

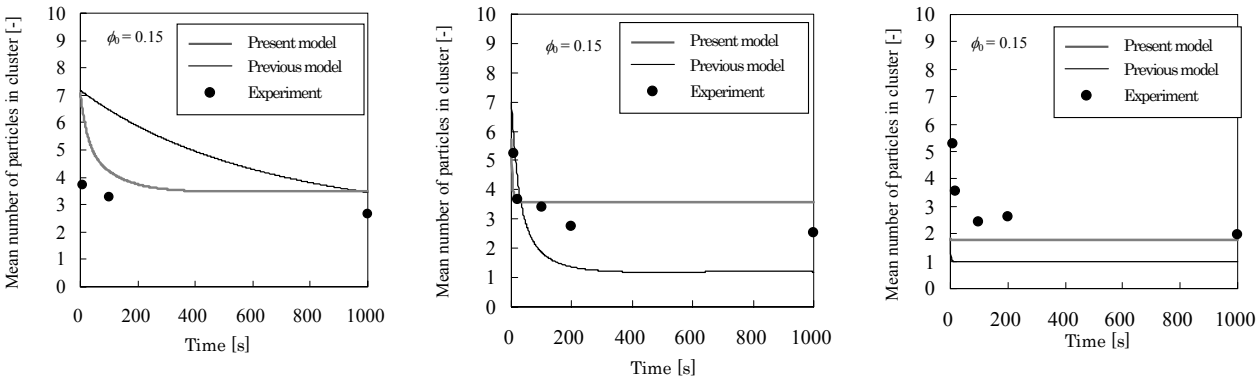

(a) $\dot{\gamma}$ = 0.2 s^{-1} (b) $\dot{\gamma}$ = 1.0 s^{-1} (c) $\dot{\gamma}$ = 10 s^{-1}

Fig. 6. Time-variations of mean cluster size when $\phi_0 = 0.15$ (a) $\dot{\gamma}$ = 0.2 s^{-1}, (b) $\dot{\gamma}$ = 1.0 s^{-1}, (c) $\dot{\gamma}$ = 10 s^{-1}.

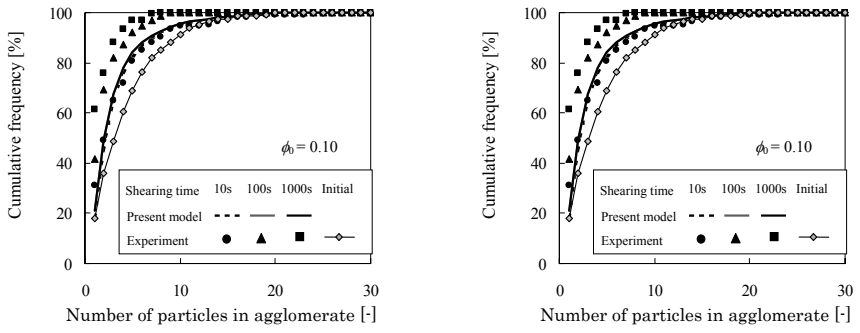

(a) ϕ_0 = 0.10 (b) ϕ_0 = 0.25

Fig. 7. Cumulative cluster size distributions when $\dot{\gamma}$ = 1.0 s^{-1} (a) ϕ_0 = 0.10, (b) ϕ_0 = 0.25.

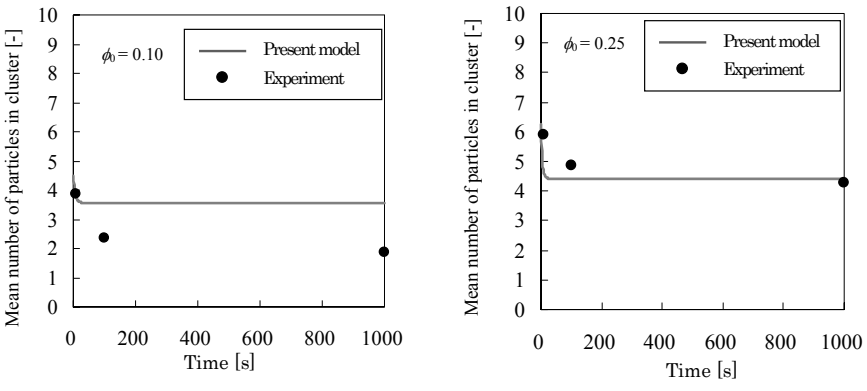

(a) ϕ_0 = 0.10 (b) ϕ_0 = 0.25

Fig. 8. Time-variations of mean cluster size when $\dot{\gamma}$ = 1.0 s^{-1} (a) ϕ_0 = 0.10, (b) ϕ_0 = 0.25.

with the experimental data.

The mean cluster size at 1000 s in each case is plotted in Figure 9. In this figure, the mean cluster size calculated with Usui's model is also plotted. The estimation of mean cluster size with Usui's model was performed with a constant bonding energy as reported in the previous study.

From this, it is found that the mean cluster size with Usui's model decreases with volume fraction. The mean cluster size with Usui's model is calculated as the viscosity estimated with Simha's model agrees with the experimental result. Then, the cluster size obtained by Usui's model shows significant disagreement. When the present model is used, the mean cluster size increases with volume fraction. Though it is slightly higher than the experimental data in the case when $\phi_0 = 0.10$, the increase tendency of the mean cluster size with volume fraction qualitatively agrees with experimental data.

Figure 10 shows the viscosity at 1000 s for each case. From this, Usui's model well agrees with the experimental result in each case. This is because the cluster size is decided as the viscosity agrees with experimental data in the Usui's model.

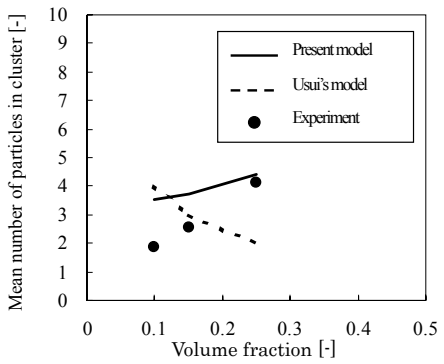

Fig. 9. Mean cluster size at 1000 s.

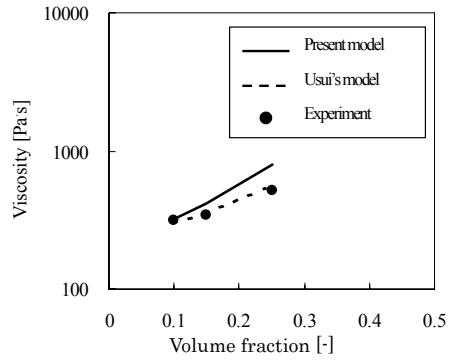

Fig. 10. Viscosity at 1000 s.

Though the viscosities obtained by the present model show slightly higher values than the experimental data, it is found that they agrees rather well in spite of the fact that only the initial distribution of cluster size was used.

4. CONCLUSIONS

In this paper, a model estimating the time-dependent distribution of cluster size consisting of fine particles in a Newtonian fluid proposed in the previous study was improved. The present model assumed interparticle bonding energy is a function of cluster size when a cluster size is small. The viscosity model was changed from Simha's to Eilers' models.

From the comparison with experimental data, the present model was found to express the time variation characteristics of viscosity and cluster size distribution rather well. It was valid in a range of the volume fraction ranges from 0.10 to 0.25.

Notation

b_{ij} coagulation rate , $m^3 \cdot s^{-1}$
d_0 diameter of particles, m
d_k cluster diameter, m
F_0 bonding energy, J
k number of particles in a cluster, dimensionless
k_b Boltzmann constant, $J \cdot K^{-1}$
N_0 total number of the primary particles per unit volume, dimensionless
N_b number of bonds to be broken when the cluster is divided, dimensionless
n_k concentration of the clusters composed of k particles, m^{-3}
r_i radii of the clusters including i particles, m
T absolute temperature, K
t time, s
α_b, α_s Brownian and shear coagulation constants, dimensionless
γ ratio of cell radius to particle radius
$\dot{\gamma}$ shear rate, s^{-1}
ε void fraction in a cluster, dimensionless
ε_{max} maximum void fraction, dimensionless
η, η_0 slurry and solvent viscosities, Pa·s
λ coefficient on the volume fraction, dimensionless
ϕ, ϕ_0 apparent and actual solid volume fractions, dimensionless
ϕ_{pmax} maximum solid volume fraction

REFERENCES

1) Smoluchowski M, *Z Phys Chem*, **92**, 129-168 (1917).
2) Swift DL, Friedlander SK, *J Colloid Sci*, **19**, 621-647 (1964).
3) Friedlander SK, Wang CS, *J Colloid Interfaces Sci*, **22**, 126-132 (1966).
4) Higashitani K, Tanaka T, Matsuno Y, *J Colloid Interfaces Sci*, **63(3)**, 551-560 (1978).
5) Higashitani K, Miyafusa S, Matsuda T, Matsuno Y, *J Colloid Interfaces Sci*, **77(1)**, 21-28 (1980).
6) Higashitani K, Ogawa R, Hosokawa G, Matsuno Y, *J Chem Eng Jpn*, **15(4)**, 299-304 (1982).
7) Parker DS, Kaufman WJ, Jenkins D, *Journal of the Sanitary Engineering Division*, **98(SA1)**, 79-99 (1972).
8) Sonntag RC, Russel WB, *J Colloid Interfaces Sci*, **113(2)**, 399-413(1986).
9) Usui H, *Kagaku Kougaku Ronbunshu*, **25**, 459-495 (1999).
10) Usui H, Kishimoto K, Suzuki H, *Chem Eng Sci*, **56**, 2979-2989 (2001).
11) Usui H, Li L, Kinoshita S, Suzuki H, *J Chem Eng Jpn*, **34(3)**, 360-368 (2001).
12) Mustafa, Usui H, Ibuki S, Suzuki H, Kobayashi T, Miyazaki Y, Ioroi T, Yasuda K, *J Chem Eng Jpn*, **37(1)**, 31-39 (2004).
13) Komoda Y, Nakashima K, Suzuki H, Usui H, *Adv Powder Tech*, **17(3)**, 333-343, (2006).
14) Kobayashi M, Adachi Y, Ooi S, *Langmuir*, **15**, 4351-4356 (1999).
15) Komoda Y, Kameyama K, Hasegawa E, Suzuki H, Usui H, Endo Y, Syudo A, *Adv Powder Tech*, in press.
16) Komoda Y, Kameyama K, Hasegawa E, Suzuki H, Usui H, *Nihon Reoroji Gakkaishi (J Soc Rheol, Jpn)*, in press.
17) Hasegawa E, Suzuki H, Kameyama K, Komoda Y, Usui H, *Adv Powder Tech*, in press.
18) Simha R, *J App Phys*, **23**, 1020-1024 (1952).
19) Einstein A, *Investigation on the Theory of the Brownian Movement*, Dover, New York (1956).
20) Eilers H, Kolloid Zh, **97**, 313-321(1941).